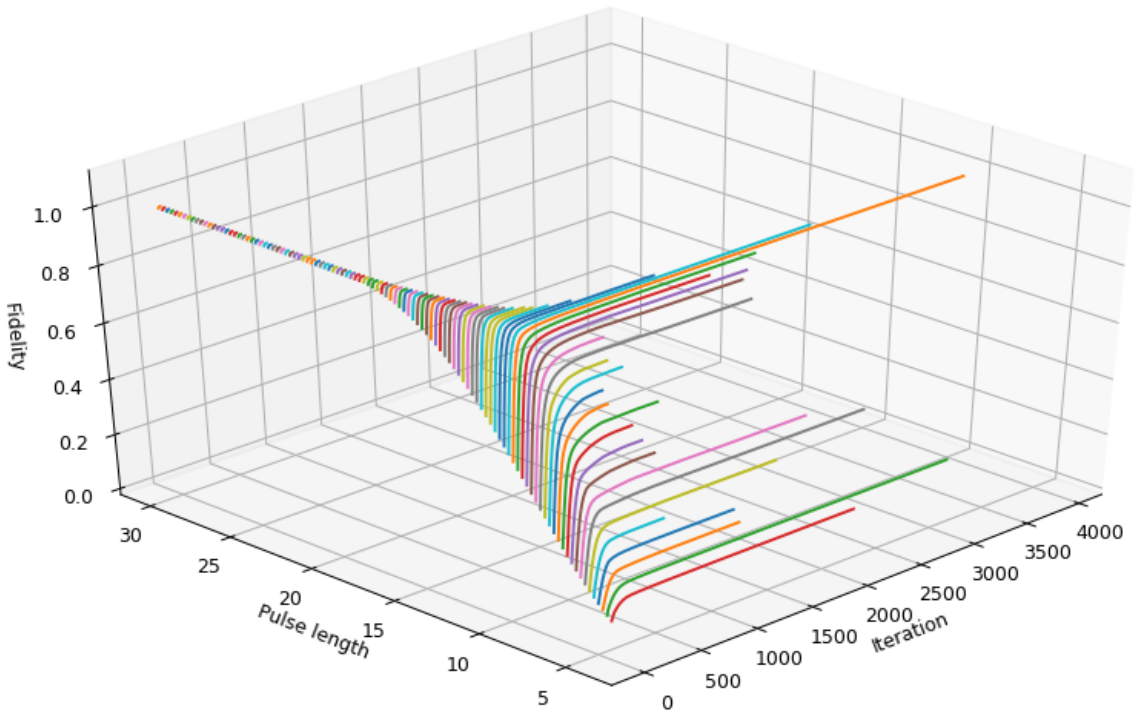

Figure 1.1: *Fidelity during optimisations for every pulse length (ns). The different colors help distinguish the lines.*

1 Results

The results of the numerical experiments will be presented in this chapter. For both optimisation targets the optimised pulses, their properties and the final evolved state will be presented.

1.1 $|0\rangle \rightarrow |1\rangle$ state transfer

In fig. 1.1 the fidelity during all optimisation runs are plotted. For pulse lengths longer than 15 ns the fidelity starts at values close to the goal ($F > 0.9$) and the number of iterations is low (less than 85 iterations). In contrast, pulses shorter than 15 ns start at lower fidelities while the number of iterations are roughly one order of magnitude larger with no clear pattern.

To give more detail, the start and end fidelity over pulse length is plotted in fig. 1.2. The optimisations where the fidelity goal was not reached are marked with stars which is all pulse lengths equal to and below 10.50 ns. The drop-off in fidelity for shorter pulses is linear.

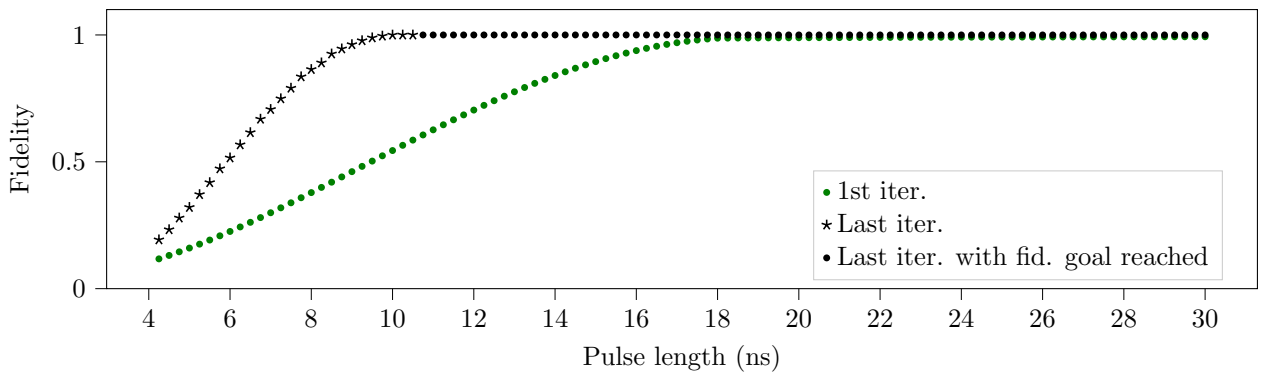

Figure 1.2: *Fidelity of first and last iteration of every pulse length. The stable region above*

Further analysis is done on pulses with lengths 4.25 ns, 6.0 ns, 8.0 ns, 10.0 ns, 20.0 ns and 30.0 ns. The optimised pulse shapes $\mathrm{Re}(\Omega)$ and $\mathrm{Im}(\Omega)$ are plotted in fig. 1.3 together with the guess pulses. Pulses longer than 20 ns require only fine adjustments to the Blackman guess pulse while shorter pulses have an imaginary part which is maximised for the whole duration of the pulse.

The spectrum of $\Omega(t)$ in the lab frame $\Omega(t)\mathrm{e}^{i\omega_{01}t}$ is shown in fig. 1.4. For all pulse lengths there is a peak centered roughly at ω_{01} and the width of the peak becomes narrower for longer pulses. For the pulse length 30 ns there is almost no support at ω_{02} and ω_{12}.

1.2 $|0\rangle \rightarrow |2\rangle$ state transfer

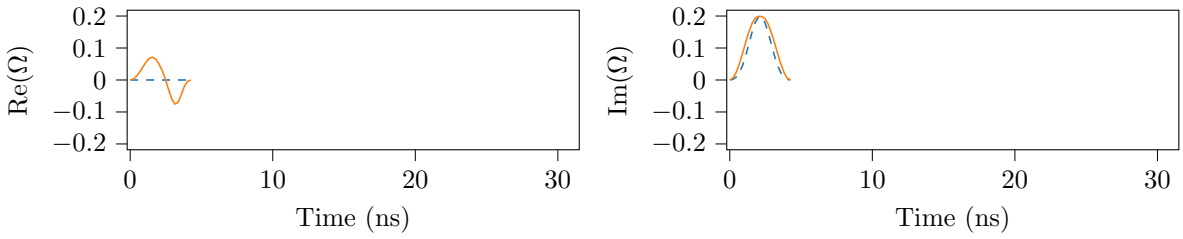

(a) *Pulse length 4.25 ns*

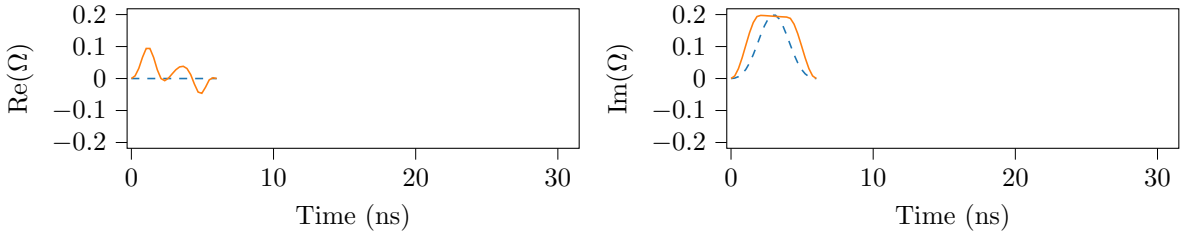

(b) *Pulse length 6.0 ns*

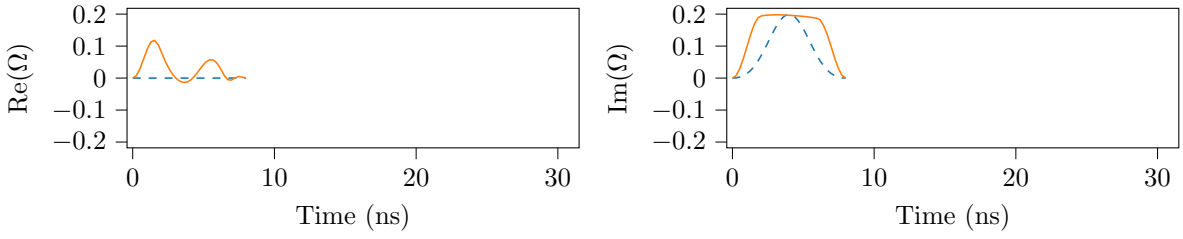

(c) *Pulse length 8.0 ns*

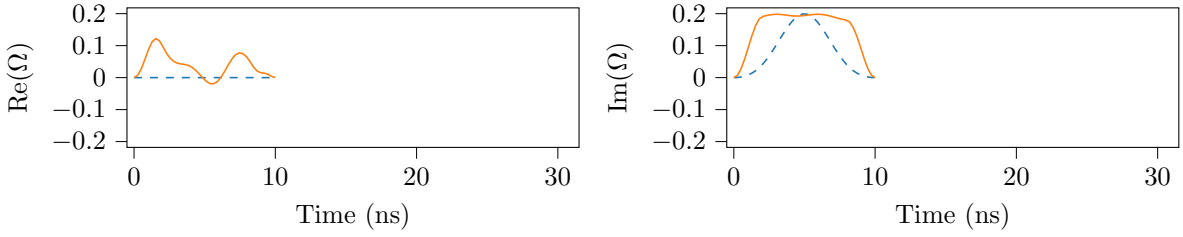

(d) *Pulse length 10.0 ns*

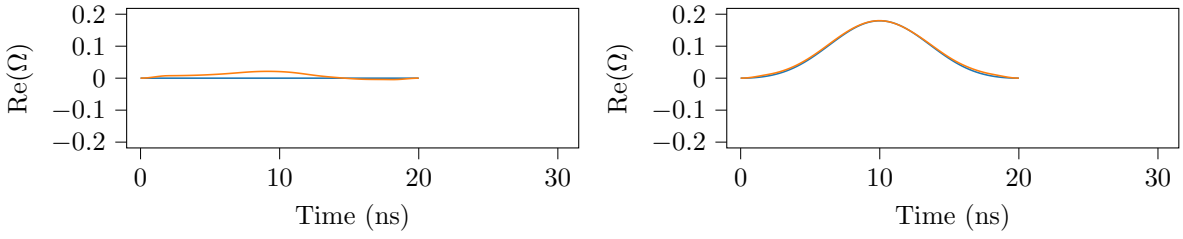

(e) *Pulse length 20.0 ns*

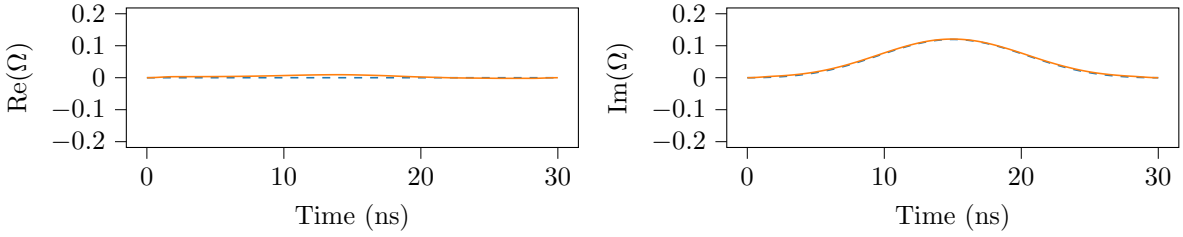

(f) *Pulse length 30.0 ns*

Figure 1.3: *Optimised pulse shapes and guess pulses for pulse lengths* **(a)** 4.25 ns, **(b)** 6.0 ns, **(c)** 8.0 ns, **(d)** 10.0 ns, **(e)** 20.0 ns, *and* **(f)** 30.0 ns. *Short pulses (*<10 ns*) change substantially from the starting Blackman shape while long pulses (*>20 ns*) only require fine adjustments.*

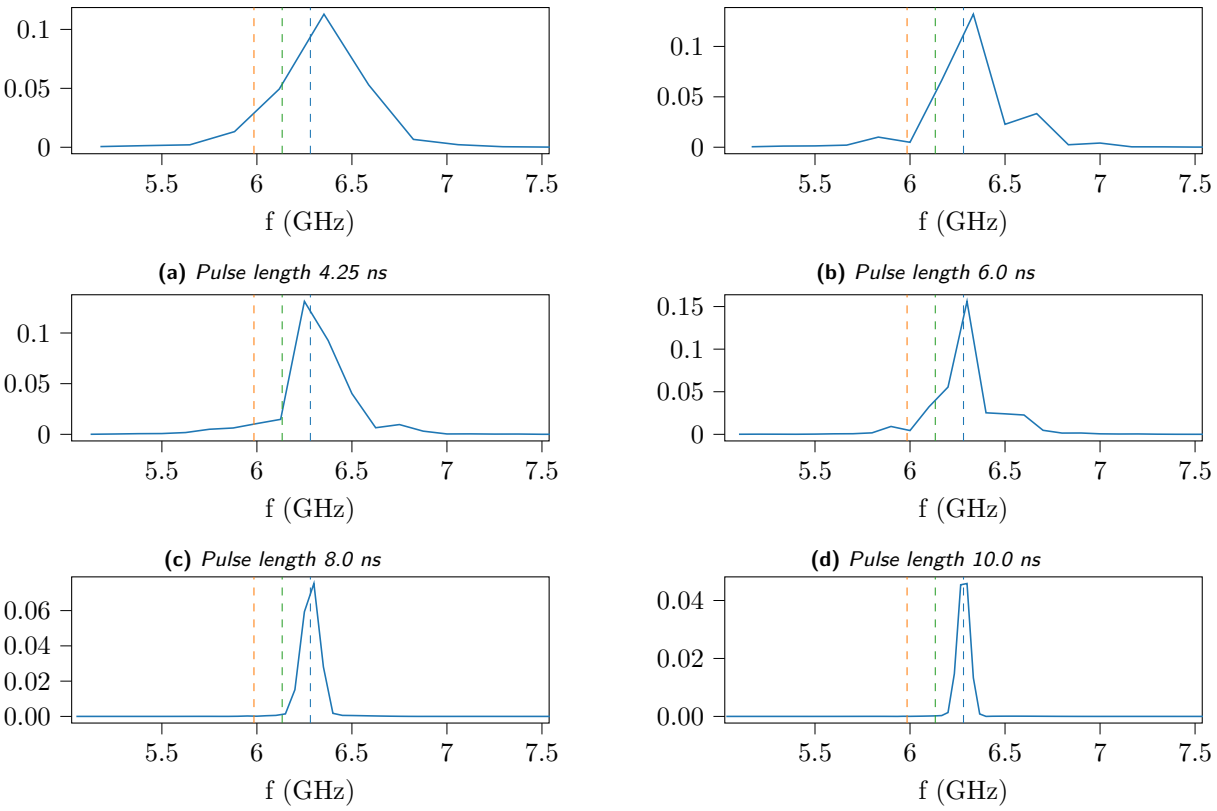

(a) *Pulse length 4.25 ns*

(b) *Pulse length 6.0 ns*

(c) *Pulse length 8.0 ns*

(d) *Pulse length 10.0 ns*

(e) *Pulse length 20.0 ns*

(f) *Pulse length 30.0 ns*

Figure 1.4: *Pulse spectrum of the complex pulses in fig. 1.3. The vertical lines indicate (from left to right)* ω_{02}, ω_{12}, ω_{01}.

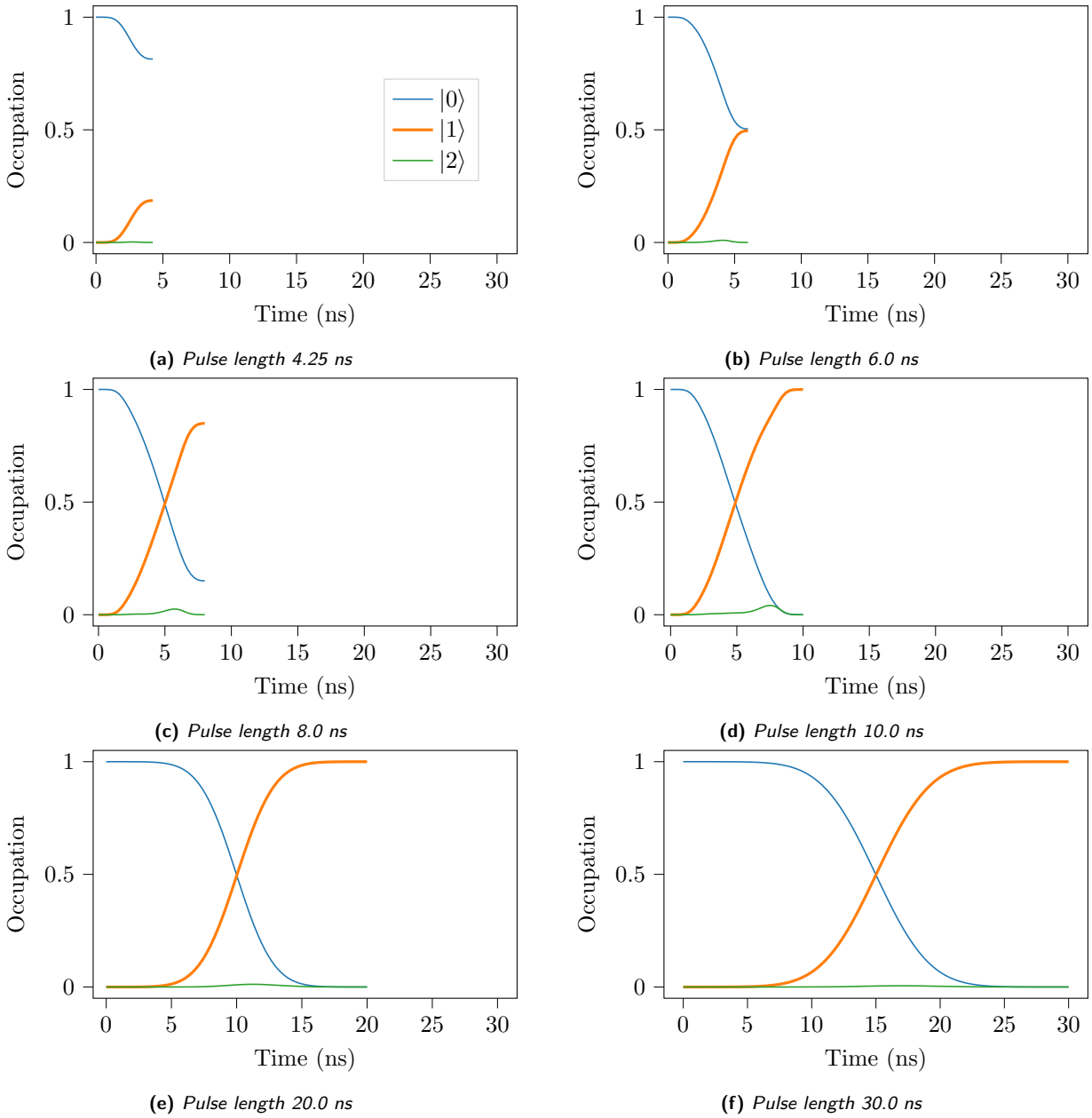

(a) *Pulse length 4.25 ns*

(b) *Pulse length 6.0 ns*

(c) *Pulse length 8.0 ns*

(d) *Pulse length 10.0 ns*

(e) *Pulse length 20.0 ns*

(f) *Pulse length 30.0 ns*

Figure 1.5: *Energy level occupation over time for different lengths of optimised pulses.*

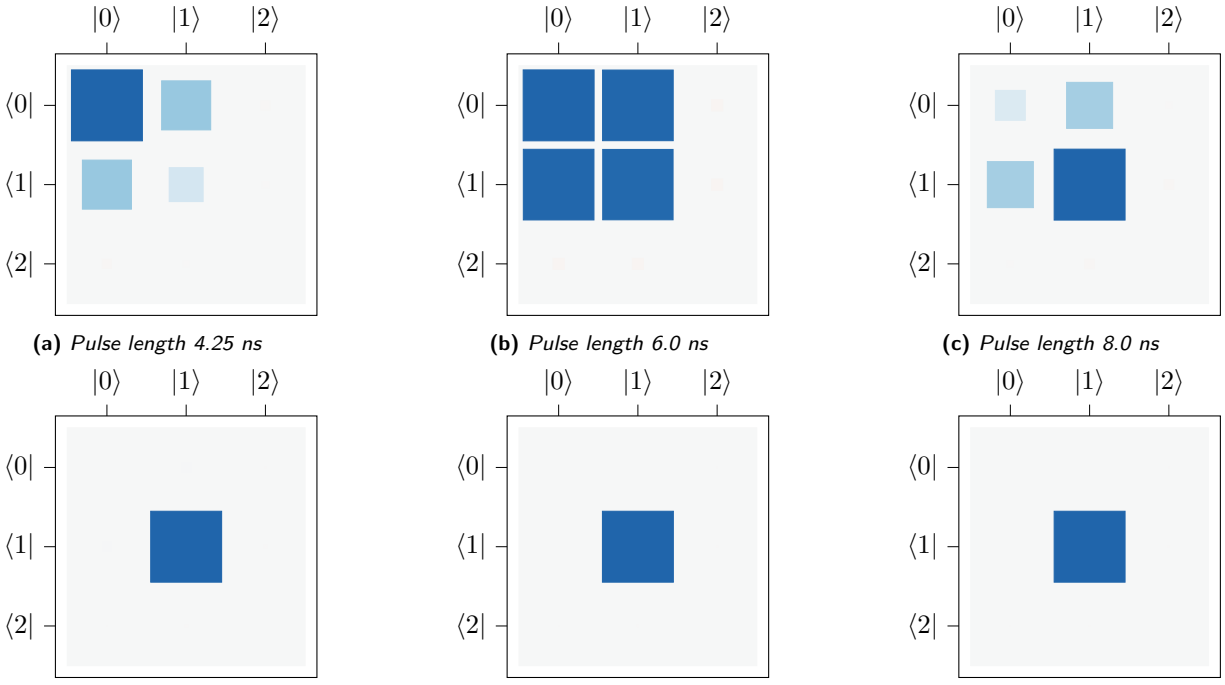

(a) *Pulse length 4.25 ns* **(b)** *Pulse length 6.0 ns* **(c)** *Pulse length 8.0 ns*

(d) *Pulse length 10.0 ns* **(e)** *Pulse length 20.0 ns* **(f)** *Pulse length 30.0 ns*

Figure 1.6: *Hinton diagram of* $|\psi(T)\rangle\langle\psi(T)|$

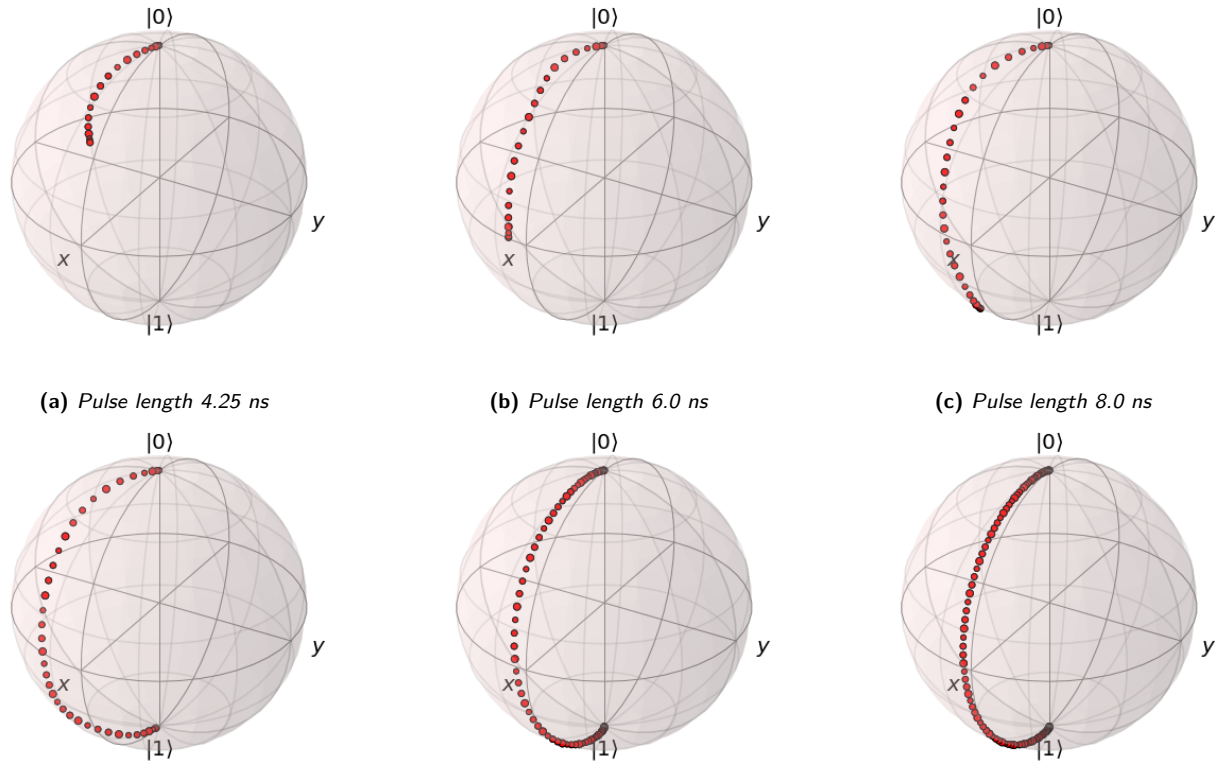

(a) *Pulse length 4.25 ns* **(b)** *Pulse length 6.0 ns* **(c)** *Pulse length 8.0 ns*

(d) *Pulse length 10.0 ns* **(e)** *Pulse length 20.0 ns* **(f)** *Pulse length 30.0 ns*

Figure 1.7: *Time dynamics on the Bloch sphere for different lengths of optimised pulses.*

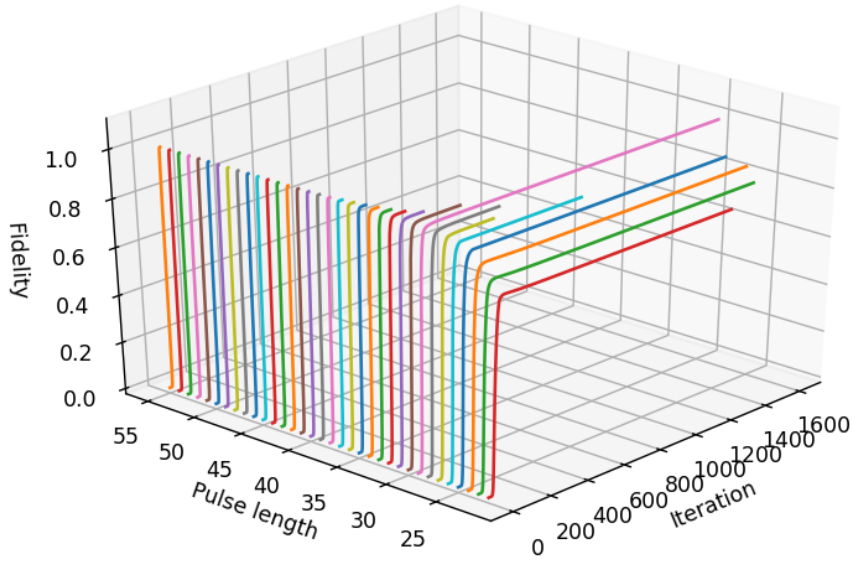

Figure 1.8: *Fidelity during optimisations for every pulse length (ns).*

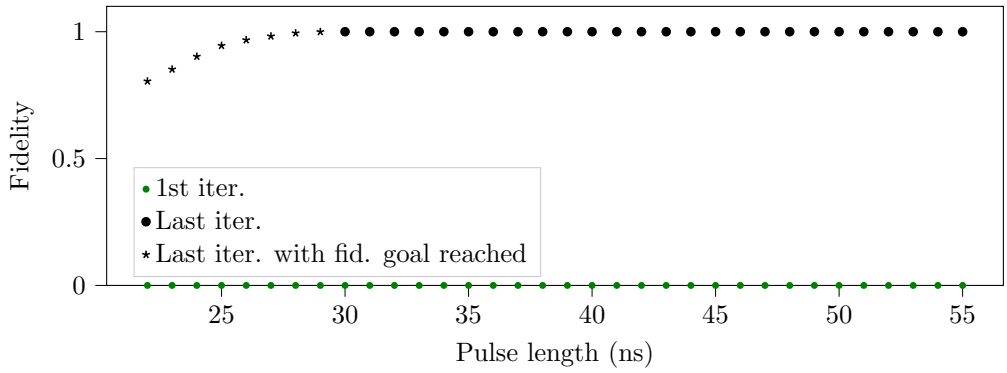

Figure 1.9: *Fidelity of first and last iteration of every pulse length.*

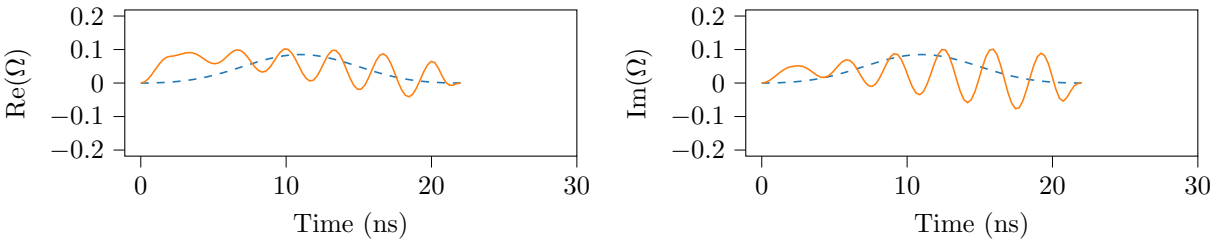

(a) *Pulse length 22.0 ns*

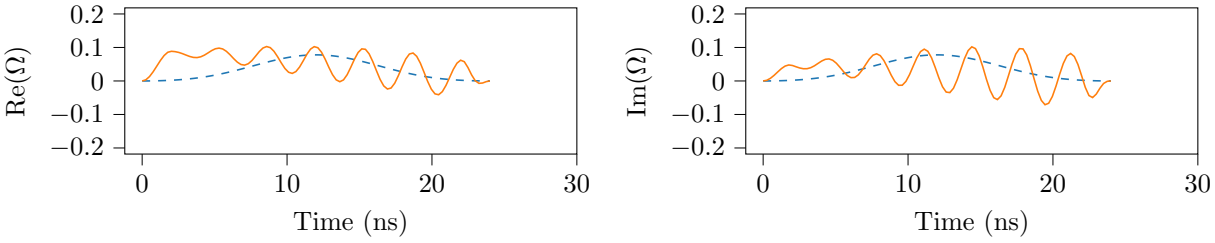

(b) *Pulse length 24.0 ns*

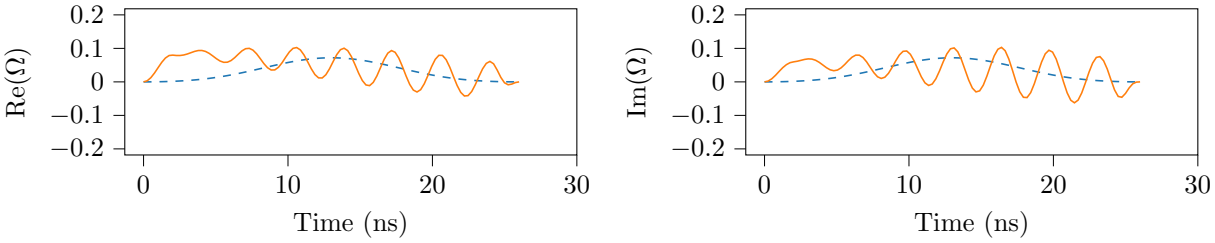

(c) *Pulse length 26.0 ns*

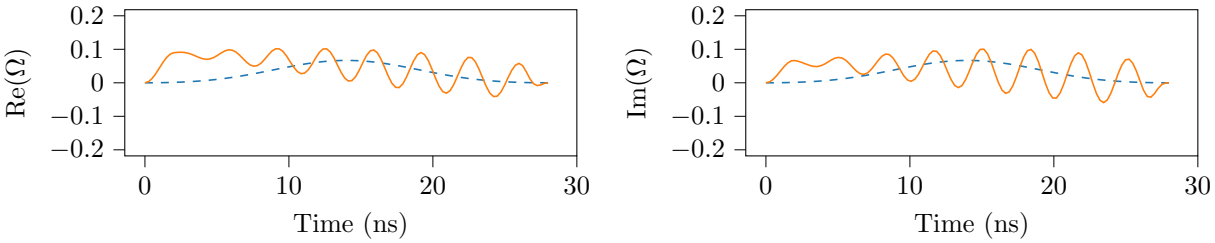

(d) *Pulse length 28.0 ns*

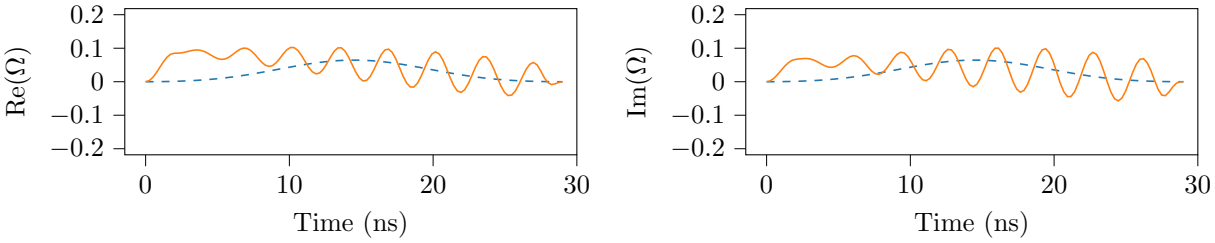

(e) *Pulse length 29.0 ns*

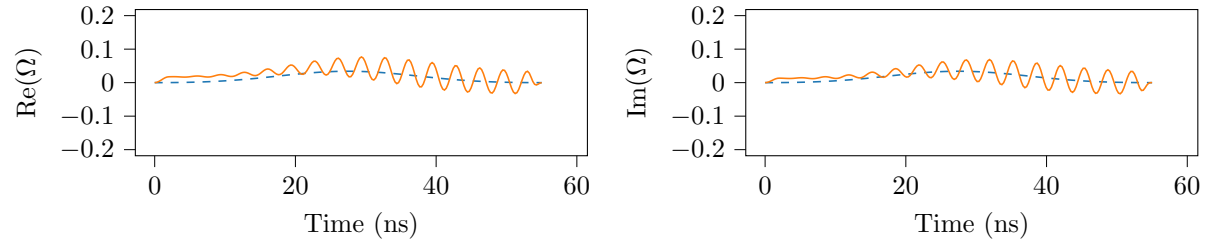

(f) *Pulse length 55.0 ns*

Figure 1.10: *Pulse shapes.*

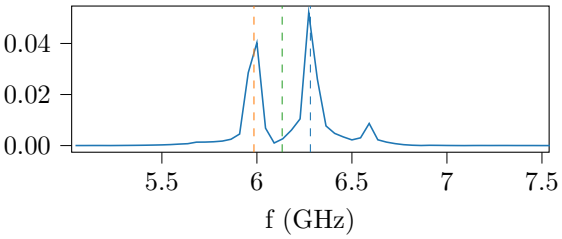

(a) *Pulse length 22.0 ns*

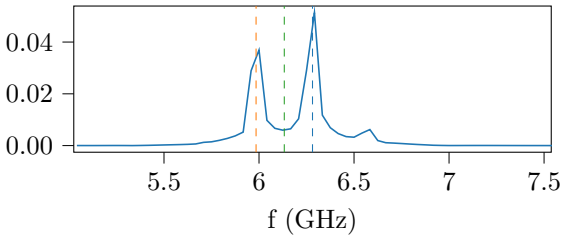

(b) *Pulse length 24.0 ns*

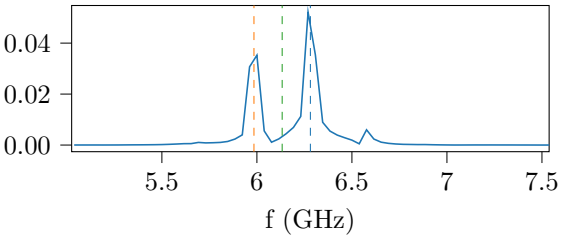

(c) *Pulse length 26.0 ns*

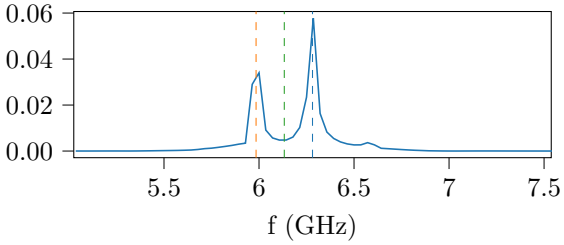

(d) *Pulse length 28.0 ns*

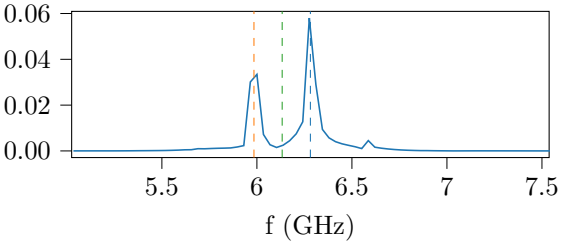

(e) *Pulse length 29.0 ns*

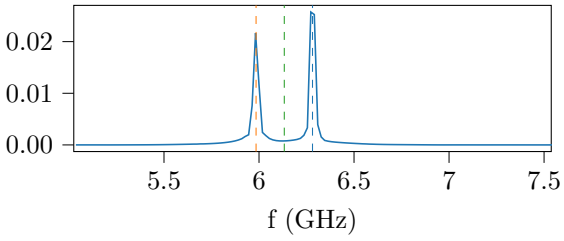

(f) *Pulse length 55.0 ns*

Figure 1.11: *Pulse spectrum*

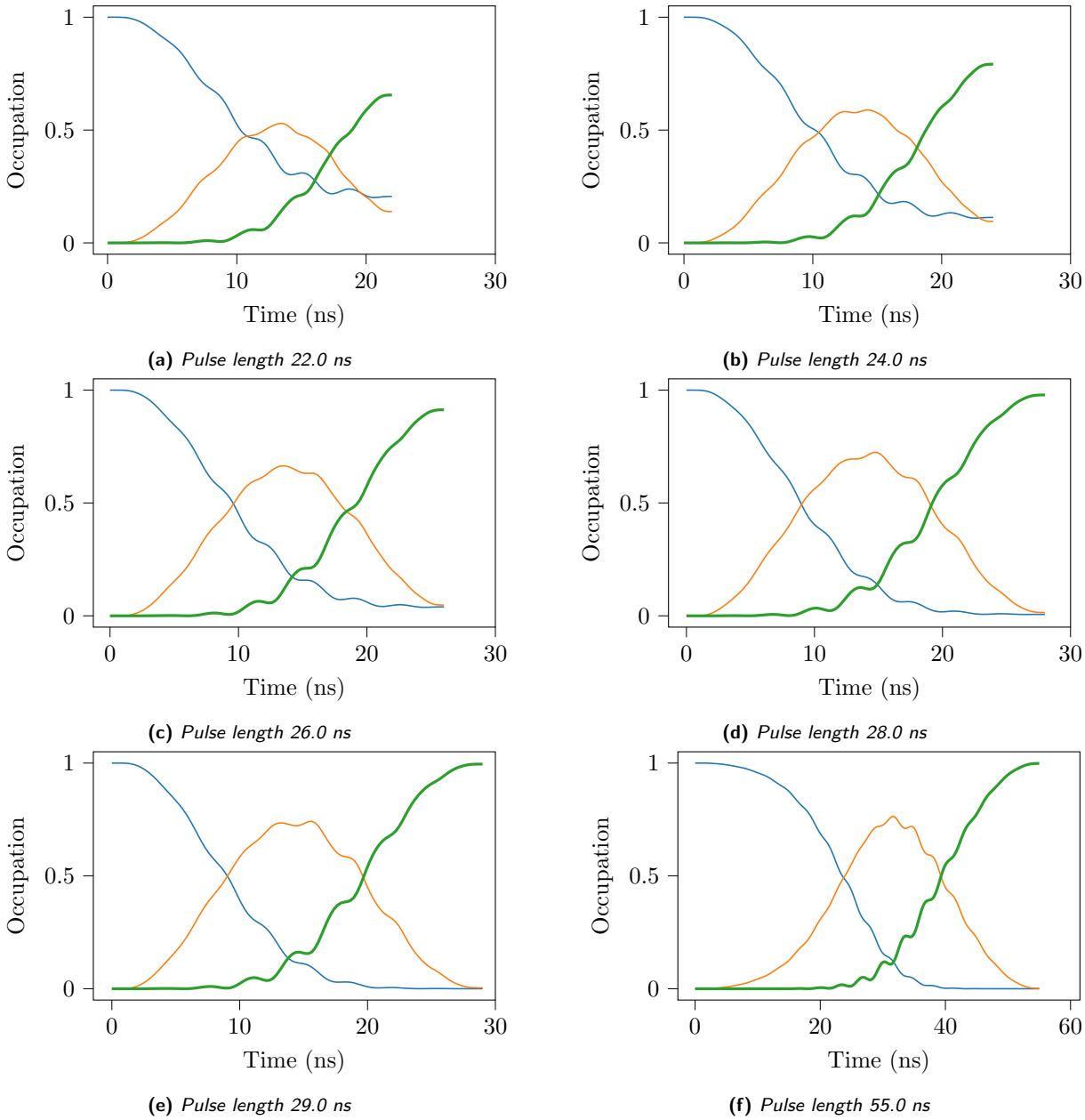

(a) *Pulse length 22.0 ns*

(b) *Pulse length 24.0 ns*

(c) *Pulse length 26.0 ns*

(d) *Pulse length 28.0 ns*

(e) *Pulse length 29.0 ns*

(f) *Pulse length 55.0 ns*

Figure 1.12: *Energy level occupation over time for different lengths of optimised pulses.*

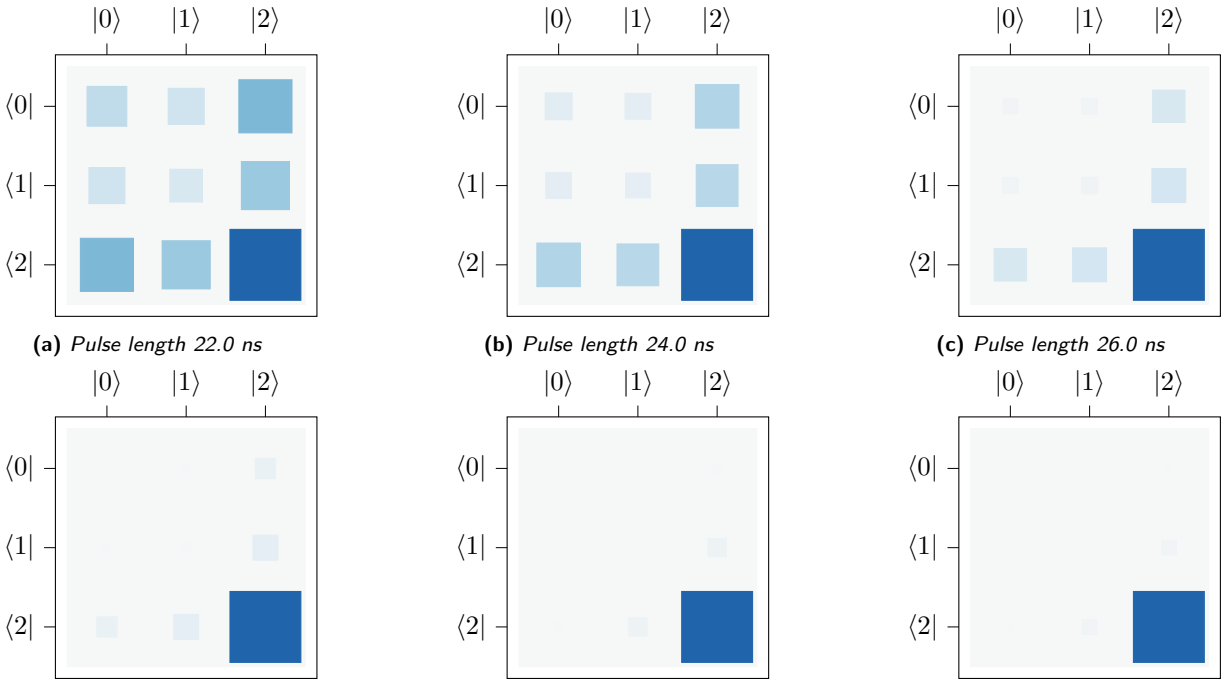

(a) *Pulse length 22.0 ns* **(b)** *Pulse length 24.0 ns* **(c)** *Pulse length 26.0 ns*

(d) *Pulse length 28.0 ns* **(e)** *Pulse length 29.0 ns* **(f)** *Pulse length 55.0 ns*

Figure 1.13: *Hinton diagram of* $|\psi(T)\rangle\langle\psi(T)|$